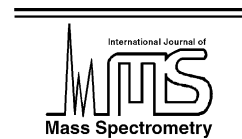




ELSEVIER

International Journal of Mass Spectrometry 222 (2003) 505–509



www.elsevier.com/locate/ijms

Subject index Volume 222

Ab initio

- On the acidity of cyclopropanaphthalenes. Gas phase and computational studies, 11
- Electron-impact total ionization cross-sections of the chloro-fluoromethanes, 189

Ab initio calculations

- Metastable states of dimethyloxonium, $(\text{CH}_3)_2\text{OH}^+$, 49
- The fluoride affinity of SO_2 , 221

Activation entropies

- Protonation thermochemistry of β -alanine. An evaluation of proton affinities and entropies determined by the extended kinetic method, 465

Adduct ion formation

- Chemical ionization of amino and hydroxy group containing arylalkyl compounds with ions in a nitromethane plasma, 101

Alkali metal ions

- Influence of substituents on cation– π interactions. 5. Absolute binding energies of alkali metal cation–anisole complexes determined by threshold collision-induced dissociation and theoretical studies, 431

Allylic cation

- Taming halonium metathesis, 451

Amide

- Ligand exchange reactions of proton bound dimers of carbox-amides models for protonated proteins, 27

Amino acids

- Chiral recognition of non-natural α -amino acids, 259
- Protonation thermochemistry of β -alanine. An evaluation of proton affinities and entropies determined by the extended kinetic method, 465

Ammonia

- Collision-induced dissociation and theoretical studies of K^+ complexes with ammonia: a test of theory for potassium ions, 329

Anhydride

- The mechanism of C-terminal fragmentations in alkali metal ion complexes of peptides, 117

Antiaromaticity

- On the acidity of cyclopropanaphthalenes. Gas phase and computational studies, 11

Arginine residues

- Involvement of salt bridges in a novel gas phase rearrangement of protonated arginine-containing dipeptides which precedes fragmentation, 229

Aromaticity

- On the acidity of cyclopropanaphthalenes. Gas phase and computational studies, 11

Art

- Identification of colorants as used in watercolor and oil paintings by UV laser desorption mass spectrometry, 85

Arylalkylamines

- Chemical ionization of amino and hydroxy group containing arylalkyl compounds with ions in a nitromethane plasma, 101

Basic peptides

- A comparison of negative and positive ion time-of-flight post-source decay mass spectrometry for peptides containing basic residues, 363

BEE geometry

- Time-resolved kinetic energy releases in propane, 213

Biological matrix

- Quantification and confirmation of identity of analytes in various matrices with in-source collision-induced dissociation on a single quadrupole mass spectrometer, 281

Bond dissociation energies

- Collision-induced dissociation and theoretical studies of K^+ complexes with ammonia: a test of theory for potassium ions, 329

- Influence of substituents on cation– π interactions. 5. Absolute binding energies of alkali metal cation–anisole complexes determined by threshold collision-induced dissociation and theoretical studies, 431

Boundary activation

- Matrix-assisted laser desorption/ionization—boundary-activated dissociation of peptide ions in a quadrupole ion trap, 75

Cation– π interactions

- Influence of substituents on cation– π interactions. 5. Absolute binding energies of alkali metal cation–anisole complexes determined by threshold collision-induced dissociation and theoretical studies, 431

Charge transfer

- Reactions of O_2^+ , NO^+ and H_3O^+ with methylcyclohexane (C_7H_{14}) and cyclooctane (C_8H_{16}) from 298 to 700 K, 413

Chemical ionization

- Chemical ionization of amino and hydroxy group containing arylalkyl compounds with ions in a nitromethane plasma, 101

- Chemical mass shifts
Chemical mass shifts in quadrupole ion traps as analytical characteristics of nitro-aromatic compounds, 481
- Chiral recognition
Chiral recognition of non-natural α -amino acids, 259
- Chlorofluorocarbon
Electron-impact total ionization cross-sections of the chlorofluoromethanes, 189
- CID
The fluoride affinity of SO_2 , 221
The energetics of nitric oxide generation upon protonation of diazeniumdiolates, 269
- Clusters
Ligand exchange reactions of proton bound dimers of carboxamides models for protonated proteins, 27
- Collision-induced dissociation
Collision-induced dissociation and theoretical studies of K^+ complexes with ammonia: a test of theory for potassium ions, 329
Influence of substituents on cation– π interactions. 5. Absolute binding energies of alkali metal cation–anisole complexes determined by threshold collision-induced dissociation and theoretical studies, 431
Chemical mass shifts in quadrupole ion traps as analytical characteristics of nitro-aromatic compounds, 481
- Computer modeling
Modeling the ion density distribution in collisional cooling RF multipole ion guides, 155
- Confirmation of identity
Quantification and confirmation of identity of analytes in various matrices with in-source collision-induced dissociation on a single quadrupole mass spectrometer, 281
- Covalent and non-covalent ion structures
Chemical ionization of amino and hydroxy group containing arylalkyl compounds with ions in a nitromethane plasma, 101
- Cycloalkanes
Reactions of O_2^+ , NO^+ and H_3O^+ with methylcyclohexane (C_7H_{14}) and cyclooctane (C_8H_{16}) from 298 to 700 K, 413
- Cyclodextrin
Chiral recognition of non-natural α -amino acids, 259
- Cyclopentadienyl cation
Taming halonium metathesis, 451
- Cycloproparenes
On the acidity of cyclopropanaphthalenes. Gas phase and computational studies, 11
- DFT calculations
On the acidity of cyclopropanaphthalenes. Gas phase and computational studies, 11
- Diamines
Protonation thermochemistry of β -alanine. An evaluation of proton affinities and entropies determined by the extended kinetic method, 465
- Diastereoisomeric differentiation
Theoretical interpretation of the observed diastereoisomeric differentiation of *cis*- and *trans*-2-methylcyclohexanol in the gas phase mediated by scandium(I), 383
- Diolate ions
The energetics of nitric oxide generation upon protonation of diazeniumdiolates, 269
- Dissociation
Reactions of O_2^+ , NO^+ and H_3O^+ with methylcyclohexane (C_7H_{14}) and cyclooctane (C_8H_{16}) from 298 to 700 K, 413
- Dissociation mass spectra
The water-solvated methanol ion and its isomers: experiment and theory, 41
- Dyes
Identification of colorants as used in watercolor and oil paintings by UV laser desorption mass spectrometry, 85
- Effective core potential
Electron-impact total ionization cross-sections of the chlorofluoromethanes, 189
- Electron capture mass spectrometry
Effects of oxygen and water on the resonance electron capture reactions of low electron affinity compounds, 201
- Electron impact
Electron-impact total ionization cross-sections of the chlorofluoromethanes, 189
- Electrospray ionization
Performance of a quadrupole ion trap mass spectrometer adapted for ion/ion reaction studies, 243
Space charge effects on mass accuracy for multiply charged ions in ESI–FTICR, 351
- ESI
A mass spectrometric study of noncovalent gas phase interaction of staphylococcal nucleases with 5'-nucleoside phosphate inhibitors, 397
- Excited states
Metastable states of dimethyloxonium, $(\text{CH}_3)_2\text{OH}^*$, 49
- Explosives monitoring
Chemical mass shifts in quadrupole ion traps as analytical characteristics of nitro-aromatic compounds, 481
- Finite Heat Bath Theory
Time-resolved kinetic energy releases in propane, 213
- Fluoride affinity
The fluoride affinity of SO_2 , 221
- Fluorine compound
Loss of HF from $\text{C}_2\text{H}_4\text{FO}^+$ produced from 2-hydroxy-2-trifluoromethylpropanoic acid upon electron ionization, 1
- Fragmentation
Loss of HF from $\text{C}_2\text{H}_4\text{FO}^+$ produced from 2-hydroxy-2-trifluoromethylpropanoic acid upon electron ionization, 1
The mechanism of C-terminal fragmentations in alkali metal ion complexes of peptides, 117
- Fragmentation energetics
Energetics of selective cleavage at acidic residues studied by time- and energy-resolved surface-induced dissociation in FTICR MS, 313
- FTICR MS
Determination of phosphate position in hexose monosaccharides using an FTICR mass spectrometer: ion/molecule reactions, labeling studies, and dissociation mechanisms, 135

- FT-ICR spectroscopy
Ligand exchange reactions of proton bound dimers of carboxamides models for protonated proteins, 27
- FTMS
On the acidity of cyclopropanaphthalenes. Gas phase and computational studies, 11
A mass spectrometric study of noncovalent gas phase interaction of staphylococcal nucleases with 5'-nucleoside phosphate inhibitors, 397
- Gas-phase conformational analysis
Application of ion mobility to the gas-phase conformational analysis of polyhedral oligomeric silsesquioxanes (POSS), 63
- Guided ion beam mass spectrometry
Collision-induced dissociation and theoretical studies of K^+ complexes with ammonia: a test of theory for potassium ions, 329
- Guided ion beams
Influence of substituents on cation- π interactions. 5. Absolute binding energies of alkali metal cation-anisole complexes determined by threshold collision-induced dissociation and theoretical studies, 431
- Hammond postulate
Taming halonium metathesis, 451
- Homocubane clusters
Characterization of $\{M_8[S_2CC(CN)_2]_6\}^{4-}$, where $M = Cu^I$ and Ag^I , homocubane clusters by ^{252}Cf -plasma desorption mass spectrometry, 493
- Host-guest complexes
Chiral recognition of non-natural α -amino acids, 259
- Hydride transfer
Reactions of O_2^+ , NO^+ and H_3O^+ with methylcyclohexane (C_7H_{14}) and cyclooctane (C_8H_{16}) from 298 to 700 K, 413
- Hydrogen/deuterium exchange
Gas phase hydrogen/deuterium exchange of proteins in an ion trap mass spectrometer, 175
- Hypervalent radicals
Metastable states of dimethyloxonium, $(CH_3)_2OH^+$, 49
- Ion cooling
Modeling the ion density distribution in collisional cooling RF multipole ion guides, 155
- Ion cyclotron resonance
Space charge effects on mass accuracy for multiply charged ions in ESI-FTICR, 351
- Ion mobility
Application of ion mobility to the gas-phase conformational analysis of polyhedral oligomeric silsesquioxanes (POSS), 63
- Ion parking
Performance of a quadrupole ion trap mass spectrometer adapted for ion/ion reaction studies, 243
- Ion trap mass spectrometry
Gas phase hydrogen/deuterium exchange of proteins in an ion trap mass spectrometer, 175
- Ion/ion reactions
Performance of a quadrupole ion trap mass spectrometer adapted for ion/ion reaction studies, 243
- Ion/molecule reactions
Determination of phosphate position in hexose monosaccharides using an FTICR mass spectrometer: ion/molecule reactions, labeling studies, and dissociation mechanisms, 135
- Ion-dipole complex
Loss of HF from $C_2H_4FO^+$ produced from 2-hydroxy-2-trifluoromethylpropanoic acid upon electron ionization, 1
- Ionization cross-section
Electron-impact total ionization cross-sections of the chlorofluoromethanes, 189
- Ion-molecule reaction
Ligand exchange reactions of proton bound dimers of carboxamides models for protonated proteins, 27
Gas phase hydrogen/deuterium exchange of proteins in an ion trap mass spectrometer, 175
Taming halonium metathesis, 451
- IRMPD
Determination of phosphate position in hexose monosaccharides using an FTICR mass spectrometer: ion/molecule reactions, labeling studies, and dissociation mechanisms, 135
- K^+
Collision-induced dissociation and theoretical studies of K^+ complexes with ammonia: a test of theory for potassium ions, 329
- Kinetic energy release
Time-resolved kinetic energy releases in propane, 213
- Kinetic method
Protonation thermochemistry of β -alanine. An evaluation of proton affinities and entropies determined by the extended kinetic method, 465
- Kinetics
Ligand exchange reactions of proton bound dimers of carboxamides models for protonated proteins, 27
Reactions of O_2^+ , NO^+ and H_3O^+ with methylcyclohexane (C_7H_{14}) and cyclooctane (C_8H_{16}) from 298 to 700 K, 413
- β -Lactam antibiotics
Quantification and confirmation of identity of analytes in various matrices with in-source collision-induced dissociation on a single quadrupole mass spectrometer, 281
- Laser desorption
Identification of colorants as used in watercolor and oil paintings by UV laser desorption mass spectrometry, 85
- Ligand exchange
Ligand exchange reactions of proton bound dimers of carboxamides models for protonated proteins, 27
- Lincomycin
Quantification and confirmation of identity of analytes in various matrices with in-source collision-induced dissociation on a single quadrupole mass spectrometer, 281
- Linked scans
Time-resolved kinetic energy releases in propane, 213
- Liquid chromatography
Quantification and confirmation of identity of analytes in various matrices with in-source collision-induced dissociation on a single quadrupole mass spectrometer, 281

Lithium

The mechanism of C-terminal fragmentations in alkali metal ion complexes of peptides, 117

Low electron affinity compounds

Effects of oxygen and water on the resonance electron capture reactions of low electron affinity compounds, 201

MALDI

Matrix-assisted laser desorption/ionization—boundary-activated dissociation of peptide ions in a quadrupole ion trap, 75
A comparison of negative and positive ion time-of-flight post-source decay mass spectrometry for peptides containing basic residues, 363

Mass range

Modeling the ion density distribution in collisional cooling RF multipole ion guides, 155

Mass spectrometry

Quantification and confirmation of identity of analytes in various matrices with in-source collision-induced dissociation on a single quadrupole mass spectrometer, 281

Mechanisms

Theoretical interpretation of the observed diastereoisomeric differentiation of *cis*- and *trans*-2-methylcyclohexanol in the gas phase mediated by scandium(I), 383

Metastable ion

The water-solvated methanol ion and its isomers: experiment and theory, 41

Methomyl

Quantification and confirmation of identity of analytes in various matrices with in-source collision-induced dissociation on a single quadrupole mass spectrometer, 281

MIKE

Loss of HF from $C_2H_4FO^+$ produced from 2-hydroxy-2-trifluoromethylpropanoic acid upon electron ionization, 1

Monofluorinated carbocation

Taming halonium metathesis, 451

Monosaccharide

Determination of phosphate position in hexose monosaccharides using an FTICR mass spectrometer: ion/molecule reactions, labeling studies, and dissociation mechanisms, 135

MS/MS

Matrix-assisted laser desorption/ionization—boundary-activated dissociation of peptide ions in a quadrupole ion trap, 75

Multiply-charged ions

Performance of a quadrupole ion trap mass spectrometer adapted for ion/ion reaction studies, 243

Negative ions

A comparison of negative and positive ion time-of-flight post-source decay mass spectrometry for peptides containing basic residues, 363

Neutralization-reionization mass spectrometry

Metastable states of dimethyloxonium, $(CH_3)_2OH^+$, 49

Nitric oxide

The energetics of nitric oxide generation upon protonation of diazeniumdiolates, 269

Nitro-aromatic compounds

Chemical mass shifts in quadrupole ion traps as analytical characteristics of nitro-aromatic compounds, 481

Nitromethane plasma

Chemical ionization of amino and hydroxy group containing arylalkyl compounds with ions in a nitromethane plasma, 101

Noncovalent interactions

A mass spectrometric study of noncovalent gas phase interaction of staphylococcal nucleases with 5'-nucleoside phosphate inhibitors, 397

Non-fixed energy

Time-resolved kinetic energy releases in propane, 213

Pathway

The mechanism of C-terminal fragmentations in alkali metal ion complexes of peptides, 117

Paul ion trap

Chemical mass shifts in quadrupole ion traps as analytical characteristics of nitro-aromatic compounds, 481

Pentaanionic clusters

Characterization of $\{M_8[S_2CC(CN)_2]_6\}^{4-}$, where $M = Cu^I$ and Ag^I , homocubane clusters by ^{252}Cf -plasma desorption mass spectrometry, 493

Peptide

Matrix-assisted laser desorption/ionization—boundary-activated dissociation of peptide ions in a quadrupole ion trap, 75

The mechanism of C-terminal fragmentations in alkali metal ion complexes of peptides, 117

Phosphate linkage

Determination of phosphate position in hexose monosaccharides using an FTICR mass spectrometer: ion/molecule reactions, labeling studies, and dissociation mechanisms, 135

Phosphorylated carbohydrates

Determination of phosphate position in hexose monosaccharides using an FTICR mass spectrometer: ion/molecule reactions, labeling studies, and dissociation mechanisms, 135

Pigments

Identification of colorants as used in watercolor and oil paintings by UV laser desorption mass spectrometry, 85

Plasma

Electron-impact total ionization cross-sections of the chloro-fluoromethanes, 189

Plasma desorption mass spectrometry

Characterization of $\{M_8[S_2CC(CN)_2]_6\}^{4-}$, where $M = Cu^I$ and Ag^I , homocubane clusters by ^{252}Cf -plasma desorption mass spectrometry, 493

POSS

Application of ion mobility to the gas-phase conformational analysis of polyhedral oligomeric silsesquioxanes (POSS), 63

Post-source decay

A comparison of negative and positive ion time-of-flight post-source decay mass spectrometry for peptides containing basic residues, 363

- Potential energy surface
Loss of HF from $C_2H_4FO^+$ produced from 2-hydroxy-2-trifluoromethylpropanoic acid upon electron ionization, 1
- Propane
Time-resolved kinetic energy releases in propane, 213
- Proteins
Gas phase hydrogen/deuterium exchange of proteins in an ion trap mass spectrometer, 175
Space charge effects on mass accuracy for multiply charged ions in ESI-FTICR, 351
A mass spectrometric study of noncovalent gas phase interaction of staphylococcal nucleases with 5'-nucleoside phosphate inhibitors, 397
- Proton affinities
Protonation thermochemistry of β -alanine. An evaluation of proton affinities and entropies determined by the extended kinetic method, 465
- Proton bound dimers
Ligand exchange reactions of proton bound dimers of carboxamides models for protonated proteins, 27
- Proton transfer
Reactions of O_2^+ , NO^+ and H_3O^+ with methylcyclohexane (C_7H_{14}) and cyclooctane (C_8H_{16}) from 298 to 700 K, 413
- Protonated peptides
Involvement of salt bridges in a novel gas phase rearrangement of protonated arginine-containing dipeptides which precedes fragmentation, 229
Energetics of selective cleavage at acidic residues studied by time- and energy-resolved surface-induced dissociation in FT-ICR MS, 313
- Protonation
The energetics of nitric oxide generation upon protonation of diazeniumdiolates, 269
- Quadrupole ion trap
Matrix-assisted laser desorption/ionization—boundary-activated dissociation of peptide ions in a quadrupole ion trap, 75
Performance of a quadrupole ion trap mass spectrometer adapted for ion/ion reaction studies, 243
- Quantification
Quantification and confirmation of identity of analytes in various matrices with in-source collision-induced dissociation on a single quadrupole mass spectrometer, 281
- Ritonavir
Quantification and confirmation of identity of analytes in various matrices with in-source collision-induced dissociation on a single quadrupole mass spectrometer, 281
- RRKM modeling
Energetics of selective cleavage at acidic residues studied by time- and energy-resolved surface-induced dissociation in FT-ICR MS, 313
- Salt bridges
Involvement of salt bridges in a novel gas phase rearrangement of protonated arginine-containing dipeptides which precedes fragmentation, 229
- Scandium
Theoretical interpretation of the observed diastereoisomeric differentiation of *cis*- and *trans*-2-methylcyclohexanol in the gas phase mediated by scandium(I), 383
- sec*-Propyl cation
Time-resolved kinetic energy releases in propane, 213
- Selective cleavage
Energetics of selective cleavage at acidic residues studied by time- and energy-resolved surface-induced dissociation in FT-ICR MS, 313
- Sequencing
Involvement of salt bridges in a novel gas phase rearrangement of protonated arginine-containing dipeptides which precedes fragmentation, 229
- Simulation
Modeling the ion density distribution in collisional cooling RF multipole ion guides, 155
- Single quadrupole
Quantification and confirmation of identity of analytes in various matrices with in-source collision-induced dissociation on a single quadrupole mass spectrometer, 281
- SORI-CID
Determination of phosphate position in hexose monosaccharides using an FTICR mass spectrometer: ion/molecule reactions, labeling studies, and dissociation mechanisms, 135
- Space charge
Modeling the ion density distribution in collisional cooling RF multipole ion guides, 155
- Spontaneous and electron-induced dissociations
Time-resolved kinetic energy releases in propane, 213
- Sulfometuron methyl
Quantification and confirmation of identity of analytes in various matrices with in-source collision-induced dissociation on a single quadrupole mass spectrometer, 281
- Surface-induced dissociation
Energetics of selective cleavage at acidic residues studied by time- and energy-resolved surface-induced dissociation in FT-ICR MS, 313
- Tandem mass spectrometry
The water-solvated methanol ion and its isomers: experiment and theory, 41
Involvement of salt bridges in a novel gas phase rearrangement of protonated arginine-containing dipeptides which precedes fragmentation, 229
- Theoretical investigations
Theoretical interpretation of the observed diastereoisomeric differentiation of *cis*- and *trans*-2-methylcyclohexanol in the gas phase mediated by scandium(I), 383
- Thermodynamics
The fluoride affinity of SO_2 , 221
- Unsaturated ketone
Taming halonium metathesis, 451
- Vibronic coupling
Metastable states of dimethyloxonium, $(CH_3)_2OH^+$, 49